"Unveiling a common mechanism of apoptosis in β-cells and neurons in Friedreich's ataxia."

Igoillo-Esteve, Mariana ; Gurgul-Convey, Ewa ; Hu, Amélie ; Romagueira Bichara Dos Santos, Laila ; Abdulkarim, Baroj ; Chintawar, Satyan ; Marselli, Lorella ; Marchetti, Piero ; Jonas, Jean-Christophe ; Eizirik, Décio L ; Pandolfo, Massimo ; Cnop, Miriam

Abstract

Friedreich's ataxia (FRDA) is a neurodegenerative disorder associated with cardiomyopathy and diabetes. Effective therapies for FRDA are an urgent unmet need; there are currently no options to prevent or treat this orphan disease. FRDA is caused by reduced expression of the mitochondrial protein frataxin. We have previously demonstrated that pancreatic β-cell dysfunction and death cause diabetes in FRDA. This is secondary to mitochondrial dysfunction and apoptosis but the underlying molecular mechanisms are not known. Here we show that β-cell demise in frataxin deficiency is the consequence of oxidative stress-mediated activation of the intrinsic pathway of apoptosis. The pro-apoptotic Bcl-2 family members Bad, DP5 and Bim are the key mediators of frataxin deficiency-induced β-cell death. Importantly, the intrinsic pathway of apoptosis is also activated in FRDA patients' induced pluripotent stem cell-derived neurons. Interestingly, cAMP induction normalizes mitochondrial oxidative...

Document type : *Article de périodique (Journal article)*

HMG Advance Access published December 30, 2014

Unveiling a common mechanism of apoptosis in β-cells and neurons in Friedreich's ataxia

Mariana Igoillo-Esteve[1], Ewa Gurgul-Convey[2], Amélie Hu[3], Laila Romagueira Bichara Dos Santos[4], Baroj Abdulkarim[1], Satyan Chintawar[3], Lorella Marselli[5], Piero Marchetti[5], Jean-Christophe Jonas[4], Décio L Eizirik[1], Massimo Pandolfo[3], Miriam Cnop[1,6,*]

[1]ULB Center for Diabetes Research, Université Libre de Bruxelles, 1070, Brussels, Belgium

[2]Institute of Clinical Biochemistry, Hannover Medical School, 30625, Hannover, Germany

[3]Laboratory of Experimental Neurology, Université Libre de Bruxelles, 1070, Brussels, Belgium

[4]Institut de recherche expérimentale et clinique, Pôle d'endocrinologie, diabète et nutrition, Université Catholique de Louvain, 1200, Brussels, Belgium

[5]Department of Endocrinology and Metabolism, University of Pisa, Pisa, Italy

[6]Division of Endocrinology, Erasmus Hospital, 1070, Brussels, Belgium

[*]Correspondence to: Miriam Cnop, ULB Center for Diabetes Research, Université Libre de Bruxelles CP-618, Route de Lennik 808, 1070 Brussels, Belgium. Tel: 32.2.555.63.05; Fax: 32.2.555.62.39, Email: mcnop@ulb.ac.be

Abstract

Friedreich's ataxia is a neurodegenerative disorder associated with cardiomyopathy and diabetes. Effective therapies for Friedreich's ataxia are an urgent unmet need; there are currently no options to prevent or treat this orphan disease. Friedreich's ataxia is caused by reduced expression of the mitochondrial protein frataxin. We have previously demonstrated that pancreatic β-cell dysfunction and death cause diabetes in Friedreich's ataxia. This is secondary to mitochondrial dysfunction and apoptosis but the underlying molecular mechanisms are not known. Here we show that β-cell demise in frataxin deficiency is the consequence of oxidative stress-mediated activation of the intrinsic pathway of apoptosis. The pro-apoptotic Bcl-2 family members Bad, DP5 and Bim are the key mediators of frataxin deficiency-induced β-cell death. Importantly, the intrinsic pathway of apoptosis is also activated in Friedreich's ataxia patients' induced pluripotent stem cell-derived neurons. Interestingly, cAMP induction normalizes mitochondrial oxidative status and fully prevents activation of the intrinsic pathway of apoptosis in frataxin-deficient β-cells and neurons. This preclinical study suggests that incretin analogs hold potential to prevent/delay both diabetes and neurodegeneration in Friedreich's ataxia.

Introduction

Friedreich's ataxia (FRDA) is an autosomal recessive neurodegenerative disease caused by a GAA trinucleotide repeat expansion in the first intron of the *FXN* gene, encoding the mitochondrial protein frataxin (1). This expansion interferes with frataxin transcription by heterochromatin silencing (1, 2). FRDA patients have 5-35% of normal frataxin levels, and this is the cause of the clinical and pathophysiological features of the disease (3). FRDA is characterized by progressive gait ataxia, muscle weakness, dysarthria, and sensory loss (4). In addition to the neurological phenotype, FRDA patients have high prevalence of hypertrophic cardiomyopathy (4, 5), glucose intolerance and diabetes (6, 7).

The main neuropathological features are loss of large proprioceptive primary sensory neurons in the dorsal root ganglia, atrophy of the posterior columns and the spinocerebellar tracts in the spinal cord, severe neuronal loss in the dentate nucleus in the cerebellum, and distal axonal loss in the pyramidal tracts, with variable involvement of visual and auditory pathways (8, 9). We have recently demonstrated that pancreatic β-cell dysfunction and loss are central for diabetes development in FRDA patients (10, 11).

Frataxin is a component of the multiprotein complex that assembles iron-sulfur (Fe-S) clusters in mitochondria, where it allosterically activates the sulfur donor enzyme NSF1 and modulates iron entry in the complex. Frataxin deficiency results in decreased Fe-S biogenesis and loss of activity of Fe-S enzymes, including several subunits of complexes I, II and III of the respiratory chain, whose impairment leads to energy deficit and enhanced production of reactive oxygen species (ROS). Frataxin-deficient cells accumulate iron, mostly in mitochondria, likely as a consequence of a homeostatic mechanism trying to restore Fe-S cluster synthesis. Excess mitochondrial

iron reacts with ROS and generates toxic radicals causing oxidative damage (12-15). Cells from FRDA patients and cells rendered frataxin-deficient by RNA interference show mitochondrial dysfunction and enhanced susceptibility to ROS (16). Frataxin silencing in neuron-like cells, obtained by differentiating neuroblastoma cells, induced accumulation of ROS and apoptosis (17). We have shown that frataxin silencing in pancreatic β-cells induces mitochondrial dysfunction and apoptosis under basal condition and following metabolic or endoplasmic reticulum (ER) stress (10). Interestingly, cAMP induction by incretin analogs was protective in frataxin-deficient β-cells (10, 11).

In eukaryotic cells, apoptosis can be executed via two molecular pathways: the extrinsic and the intrinsic pathway of apoptosis (18). The latter, also called mitochondrial pathway of apoptosis, is activated in response to ER stress, DNA damage, and mitochondrial dysfunction. The propensity of cells to undergo apoptosis, known as the apostat, is determined by the balance and interactions between pro- and anti-apoptotic proteins of the Bcl-2 family (19-21). The pro-apoptotic Bcl-2 proteins are divided into BH3-only sensitizers and activators. Sensitizers are activated transcriptionally (e.g. DP5, Bik and Noxa) or by dephosphorylation (e.g. Bad) and directly bind pro-survival family members (e.g. Bcl-X_L, Bcl-2 and Bcl-2A1) causing the release of the activators (e.g. Bim, Puma and tBid). When freed in the cytoplasm the activators bind and activate pro-death binding partners such as Bax and Bak through a conformational change, leading to their translocation to the mitochondria, outer mitochondrial membrane permeabilization, cytochrome c release, activation of the initiator caspase-9 and the effector caspase-3 and execution of cell death. The usage of Bcl-2 proteins following different pro-apoptotic stimuli is context-dependent (19).

The apoptosis pathway and mediators activated by frataxin deficiency in FRDA are unknown. The aim of this study was to elucidate the molecular mechanisms of apoptosis in cell models relevant to this severe disease. Since FRDA is caused by partial frataxin deficiency (absolute deficiency being lethal), RNA interference technology allows for mechanistic studies in *in vitro* cell models (11). More recently, induced pluripotent stem cells (iPSCs), derived from FRDA patient fibroblasts, have been differentiated into neurons and cardiomyocytes (22-25). The FRDA patients' iPSC-derived neurons recapitulate the genetic basis of the disease, the decreased frataxin expression and the mitochondrial defects (25). Using these two models we presently demonstrate that cell death in FRDA is mediated by enhanced mitochondrial oxidative stress and activation of the intrinsic pathway of apoptosis. The pro-apoptotic Bcl-2 proteins Bad, DP5 and Bim are the key mediators of cell death in frataxin deficiency. Forskolin reduces mitochondrial oxidative stress and prevents activation of the intrinsic pathway of apoptosis through selective modulation of pro-apoptotic Bcl-2 proteins. Thus, cAMP induction has therapeutic potential to prevent the loss of β-cells and neurons in FRDA

Results

Frataxin deficiency in β-cells enhances mitochondrial hydrogen peroxide and hydroxyl radical formation.

We have previously demonstrated that frataxin deficiency induces mitochondrial dysfunction and sensitizes β-cells to free fatty acid (FFA)- and ER stress-induced apoptosis (10). In other cell types frataxin deficiency enhances oxidative stress (1, 3, 26, 27). To determine if this is also a characteristic of frataxin-deficient β-cells, we knocked down frataxin in clonal rat INS-1E β-cells (Fig. 1) using one of our

previously validated siRNAs (10). Frataxin silencing induced β-cell death (Fig. 1A-C) and enhanced the expression of mitochondrial superoxide dismutase (SOD2, Fig. 1D). This enzyme catalyzes the dismutation of superoxide radicals to H_2O_2 and oxygen. We therefore examined whether mitochondrial H_2O_2 production is increased, using the specific fluorescent H_2O_2 sensor HyPer. Oxidation of HyPer, selectively targeted to the mitochondria (HyPerMito, Fig. 1E), was significantly increased in frataxin-deficient β-cells in control condition and after treatment with the FFA oleate or the ER stressor brefeldin (Fig. 1E). In contrast, cytosolic H_2O_2 formation, monitored by HyPerCyto oxidation, was not modified by frataxin deficiency (Fig. 1F). H_2O_2 is converted into the highly reactive hydroxyl radical ($OH^{\bullet}$) in the presence of ferrous iron via the Fenton reaction (28). Using the fluorescent dye HPF, enhanced $OH^{\bullet}$ formation was detected in frataxin-deficient β-cells (Fig.1G). We also examined whether frataxin silencing modifies the thiol/disulfide mitochondrial redox equilibrium, by targeting the redox sensitive biosensor roGFP to the mitochondria (mt-roGFP1). This biosensor, which is much less pH-sensitive than HyPerMito (29), reports the mitochondrial glutathione (GSH) redox state, reflecting the cellular capacity to reduce oxidized protein-thiols via the thiol based redox couple GSH/GSSG (30). In line with our observation of enhanced mitochondrial ROS production in frataxin deficiency, frataxin silencing increased mitochondrial GSH oxidation (Fig. 1H). In summary, frataxin deficiency induces mitochondrial oxidative stress and apoptosis in β-cells.

Oxidative stress contributes to apoptosis in frataxin-deficient β-cells.

We next used chemical and genetic approaches to examine whether increased oxidative stress mediates β-cell death. Apoptosis induced by frataxin silencing was

partially prevented by the cell-permeable SOD/catalase mimetic MnTMPyP (31-33) and the superoxide anion scavenger Tiron (34) in control condition and after oleate (Fig. 2A, F) or brefeldin treatment (Fig. 2D). These results were confirmed by Western blot for cleaved caspase-3 (Fig. 2B-C). MnTMPyP also protected frataxin-deficient rat islet cells from oleate-induced apoptosis (Fig. 2E and Supplementary Material, Fig. S1). Mitochondrial overexpression of the H_2O_2-inactivating enzyme catalase increased catalase activity by around 20-fold (6±2 units in control cells vs 135±21 units in mitochondrial calatase overexpressing cells, n=6-11, $p<0.001$ by paired t test). Mitochondrial catalase overexpression significantly reduced the sensitivity of frataxin-deficient β-cells to brefeldin (Fig. 2G). Thus, mitochondrial oxidative stress is a key mechanism for β-cell apoptosis in FRDA.

Frataxin-deficiency activates the intrinsic pathway of apoptosis in β-cells. Mitochondrial cytochrome c release is a hallmark of activation of the intrinsic pathway of apoptosis. Frataxin silencing induced cytochrome c release in control condition and after oleate treatment (Fig. 3A-B). Treatment with the ROS scavenger MnTMPyP prevented cytochrome c release (Fig. 4), showing that oxidative stress contributes to the activation of the intrinsic pathway of apoptosis under frataxin deficiency. We next examined the pro- and anti-apoptotic proteins of the Bcl-2 family controlling this apoptosis pathway (20, 21, 35, 36). Frataxin silencing in β-cells induced the mRNA expression of the pro-apoptotic BH3-only sensitizer DP5, as well as the BH3-only activators Bim and Puma (Fig. 3C). At the protein level, frataxin deficiency induced the Bim isoforms Bim_L and Bim_S, the latter being the most pro-apoptotic Bim splice variant (37) (Fig. 3D-E and Supplementary Material, Fig. S2A-B). For DP5 and Puma there are no good antibodies available. Frataxin silencing also

activated the BH3-only sensitizer Bad by dephosphorylation (Fig. 3D-E). Frataxin deficiency did not impair the expression of the anti-apoptotic proteins Bcl-X_L or Bcl-2 in control condition or after oleate treatment (Supplementary Material, Fig. S2C-E). Instead, Bcl-X_L protein expression was induced after frataxin silencing (Supplementary Material, Fig. S2C-D), possibly as a protective mechanism to prevent β-cell demise. Taken together, these results indicate that frataxin deficiency leads to upregulation or activation of pro-apoptotic Bcl-2 proteins but not to downregulation of pro-survival ones.

The pro-apoptotic Bcl-2 proteins Bad, DP5 and Bim mediate apoptosis in frataxin-deficient β-cells.

We next examined whether Bad, DP5, Bim or Puma mediate cell death in frataxin-deficient cells. To this end, we silenced frataxin in clonal β-cells, alone or combined with Bad, DP5, Bim or Puma siRNAs, achieving more than 50% knockdown (Supplementary Material, Fig. S3). Bad knockdown reduced β-cell apoptosis in control condition and after oleate or brefeldin exposure (Fig. 5A-B). DP5 silencing prevented oleate- but not brefeldin-induced apoptosis (Fig. 5D-E), while Bim knockdown was protective against both (Fig. 5G-H). Bad, DP5 and Bim silencing also prevented oleate-induced apoptosis in frataxin-deficient primary rat β-cells (Fig. 5C, F, I). Puma knockdown was not protective for frataxin-deficient β-cells (Fig. 5J-K). The results were confirmed by Western blots for the effector caspase-3, that was significantly less activated following Bad, DP5 and Bim silencing but not after Puma knockdown (Supplementary Material, Fig. S4).

The intrinsic pathway of apoptosis is activated in iPSC-derived neurons from FRDA patients.

To evaluate if frataxin deficiency in neurons also leads to activation of the intrinsic pathway of apoptosis we differentiated fibroblast-derived iPSCs from two FRDA patients and one age-matched healthy individual into neurons. Since heterogeneous responses between clones have been reported (25), two clones were examined per individual. As described by Hick and co-workers (25), fibroblasts from FRDA patients (FA1 and FA2) had expanded GAA repeats (800/600 and 900/400, respectively), whereas the control fibroblasts (CT) had normal GAA repeats (<20). The number of repeats was unstable during reprogramming, but stabilized in iPSC clones and during differentiation. Both FRDA iPSCs clones retained pathological GAA repeat expansions, ranging between 400 and 1000 triplets, with frataxin levels reduced at all stages to 20-30% of that of control cells (25). The neuronal phenotype of iPSC-derived neurons was confirmed by morphology, expression of specific neuronal markers such as β-III-tubulin and microtubule-associated protein 2 (MAP2), and their ability to generate sodium currents, action potentials and calcium transients (25). FRDA iPSC-derived neurons were shown to have impaired mitochondrial membrane potential and delayed functional maturation (25). We confirmed that differentiated neurons from both FRDA patients showed significantly reduced frataxin protein levels as compared to control cells (Fig. 6A and E). These FRDA neurons showed significantly enhanced cleavage of the initiator caspase-9 and the effector caspase-3 (Fig. 6A-C), demonstrating that the intrinsic pathway of apoptosis is activated. In keeping with the observations in β-cells, Bim_L and Bim_S expression was increased (Fig. 6D). In one of the four patient clones (FA 1A) caspase activation and Bim induction were not observed, in keeping with reported inter-clonal variation

(25). Taken together, these results point to activation of the intrinsic pathway of apoptosis in neurons through Bim induction as occurs in β-cells.

Forskolin reduces mitochondrial oxidative stress and prevents activation of the intrinsic pathway of apoptosis in frataxin-deficient β-cells and iPSC-derived neurons from FRDA patients.

We have previously demonstrated that analogs of the incretins glucagon-like peptide-1 (GLP-1) and glucose-dependent inhibitory peptide (GIP) are protective for frataxin-deficient β-cells (10). The adenylyl cyclase stimulator forskolin reproduces this effect (10). We examined whether forskolin modifies mitochondrial oxidative stress in frataxin deficient-β-cells using the H_2O_2 fluorescent sensor HyperMito and the redox-sensitive fluorescent probe mt-roGFP1. Forskolin treatment reduced mitochondrial H_2O_2 production and restored the mitochondrial redox state of frataxin-silenced cells (Fig. 7A-B). Forskolin fully protected frataxin-deficient β-cells from apoptosis under control condition and after brefeldin exposure, as determined by caspase-3 activation (Fig. 7C-D). This was paralleled by complete restoration of Bad phosphorylation (Fig. 7C, E) and inhibition of Bim induction (Fig. 7F). Forskolin treatment also protected frataxin-deficient rat islet cells from brefeldin-induced apoptosis (Fig. 7G) and significantly reduced Bim induction (Fig. 7H and Supplementary Material, Fig. S5). Thus, cAMP induction protects frataxin deficient β-cells by reducing oxidative stress and preventing activation of the intrinsic pathway of apoptosis. We have previously shown that the GLP-1 analog exendin-4 and the GIP mimetic [D-Ala^2]-GIP protect clonal β-cells from metabolic and ER stress-induced apoptosis (10). Exendin-4 partially prevented brefeldin-induced apoptosis in frataxin-silenced rat islet cells (Supplementary Material, Fig. S6A). [D-Ala^2]-GIP and forskolin protected frataxin-

deficient human islet cells from oleate (Supplementary Material, Fig. S6B). These data show that incretin analogs are also protective in frataxin-deficient primary rat and human islets. To examine if enhanced cAMP formation is also protective in neurons from FRDA patients, iPSC-derived neurons from two FRDA patients were treated with forskolin (Fig. 7I-L). Forskolin treatment tended to reduce caspase-3 activation in individual clones (Fig. 7I) and when pooling all samples (Fig. 7J). Expression of Bim_L and Bim_S was significantly reduced by forskolin in an individual clone (Fig. 7K) and in the pooled samples (Fig. 7L). These data suggest that cAMP inducers also prevent the activation of the intrinsic pathway of apoptosis in neurons from FRDA patients.

Discussion

FRDA is a neurodegenerative disease caused by decreased frataxin expression. The main cell types affected by frataxin deficiency are neurons from the dorsal root ganglia and dentate nucleus of the cerebellum, cardiomyocytes and pancreatic β-cells (3, 10, 38). Frataxin deficiency leads to β-cell dysfunction and death (10). Reduced mitochondrial membrane potential, decreased ATP production and insulin secretion contribute to the functional β-cell defect (10). Here, we show that frataxin deficiency in β-cells induces mitochondrial oxidative stress and activates the intrinsic pathway of apoptosis. Similar to observations in other cellular models of FRDA using RNA interference or frataxin knockout mouse cells (17, 39, 40), frataxin silencing in β-cells enhanced mitochondrial SOD2 expression, mitochondrial hydrogen peroxide production, hydroxyl radical formation and increased mitochondrial GSH oxidation (Fig. 1). This is probably the consequence of respiratory chain dysfunction. Respiratory chain complexes I, II, and III need Fe-S clusters as cofactors for proper

function. Reduced Fe-S cluster formation, as a consequence of frataxin deficiency, leads to impaired electron flow and premature electron leakage from the respiratory chain. These electrons react with molecular oxygen to form superoxide, which will in turn generate hydrogen peroxide via SOD2. In the presence of iron, hydrogen peroxide is transformed in the highly toxic hydroxyl radical via the Fenton reaction (41), leading to cell damage and death. Our data demonstrate that oxidative stress causes β-cell demise since chemical and genetic approaches to scavenge ROS protect frataxin-deficient cells from apoptosis (Fig. 2). Cell death in frataxin deficiency occurs through the intrinsic pathway of apoptosis (Fig. 3), and could be prevented by ROS scavenging (Fig. 4). The pro-apoptotic Bcl-2 family members Bad, DP5 and Bim are the key mediators of the intrinsic pathway of apoptosis (Fig. 5). Palomo and colleagues (17) previously suggested that shRNA-mediated frataxin silencing in neuron-like cells induces p53-mediated upregulation of Puma and Bax and caspase-3 activation. We confirmed that frataxin silencing in β-cells induces Puma expression, but silencing this BH3-only activator was not cytoprotective suggesting that the p53-Puma pathway does not play a role in apoptosis in frataxin deficient β-cells. Importantly, we demonstrate here that the intrinsic pathway of apoptosis is also activated in iPSC-derived neurons from FRDA patients and thus identify a common mechanism of cell death in two key cell types in FRDA (Fig. 6). Patient iPSC-derived cells are an invaluable *in vitro* model to gain pathogenic insight and test the impact of novel therapies. The differentiation of iPSCs into β-cells remains challenging, with current protocols requiring transplantation into mice in order to achieve *in vivo* β-cell maturation (42).

After the identification of oxidative stress as a potential major contributor to FRDA pathology, a variety of antioxidants and stimulants of mitochondrial function were

considered as possible therapeutics. Coenzyme Q derivatives, such as idebenone, known for their ability to participate in the electron transport chain and their antioxidant properties, were tested in preclinical and clinical studies, but they did not demonstrate efficacy in modifying disease progression (43). Oxidative damage is also strongly implicated in the pathogenesis of other neurodegenerative diseases such as Huntington's disease, amyotrophic lateral sclerosis, Alzheimer's disease, stroke, and Parkinson's disease. Clinical trials using anti-oxidant molecules such as vitamin E and C and coenzyme Q derivatives also failed to demonstrate efficacy to prevent or treat oxidative stress damage in those diseases (44, 45). It has been proposed that cAMP/PKA signaling modulates redox homeostasis in β-cells (46). Here we demonstrate that forskolin treatment normalizes mitochondrial oxidative status and prevents activation of the intrinsic pathway of apoptosis in frataxin-silenced β-cells and primary islets (Fig. 7). The incretin analogs exendin-4 and [D-Ala^2]-GIP were also protective in frataxin-deficient rat and human islets. It is of great interest that forskolin also tended to protect FRDA patients' iPSC-derived neurons from apoptosis (Fig. 7). In frataxin-deficient cells the forskolin- and incretin-mediated protective effect may be the consequence of reduced oxidative stress, but additional cAMP-mediated ROS-independent protective mechanisms may also play a role. We did not evaluate the impact of forskolin treatment on mitochondrial function of frataxin-deficient cells, but it is conceivable that the normalization of mitochondrial oxidative status decreases mitochondrial damage and improves mitochondrial function.

Taken together our results suggest that cAMP induction by incretin analogs may have therapeutic potential to prevent β-cell and neuronal cell loss in FRDA. GIP and GLP-1 receptors are expressed throughout the brain, and the GLP-1 analogs exendin-4 and liraglutide have been shown to cross the blood-brain-barrier (47). Their therapeutic

potential is being considered in amyotrophic lateral sclerosis (48), Alzheimer's (49), Parkinson's (50), and Huntington's disease (51) and stroke (52, 53). This preclinical study identifies incretin analogs as a potential new treatment for FRDA, where they may be useful to prevent/delay neurodegeneration and diabetes.

Materials and Methods

Culture of INS-1E cells, primary rat β-cells, dispersed rat and human islets, and iPSC-derived neurons.

Clonal rat INS-1E cells (a kind gift from Dr C. Wollheim, Centre Médical Universitaire, Geneva, Switzerland) were cultured in RPMI 1640 medium as previously described (54, 55). Rat islets were isolated by collagenase digestion from male Wistar rats (Charles River Laboratories) housed and used following the rules of the Belgian Regulations for Animal Care, and with approval of the local Ethical committee. Islets were hand-picked under the stereomicroscope and dispersed. β-cells were purified from the dispersed rat islets by autofluorescence-activated cell sorting (FACSAria; BD Bioscience) and cultured as described (56). Human islets from non-diabetic organ donors (n=5, age 53±3 years, BMI 26±2 kg/m^2) were isolated by collagenase digestion and density gradient purification (57) in Pisa, Italy. The islets were cultured, dispersed and transfected as previously described (58). The mean percentage of β-cells of the human islet preparations was 53±6%, as determined by insulin immunofluorescence (59). For neuronal differentiation, iPSCs from two FRDA patients and one age-matched unrelated control individual were treated for 14 days with 500 ng/ml of Noggin (60). To allow the formation of neurospheres, the cells were then cultured in NBN media (neurobasal media A+B27+N2) supplemented with FGF-2 and EGF (both 20 ng/ml; Peprotech, UK). Neuronal precursors were

maintained and propagated as neurospheres as previously described (25). For neuronal differentiation, neurospheres were plated on laminin-coated glass coverslips in NBN media (without proliferating factors) containing brain-derived neurotrophic factor (BDNF) and neurotrophin 3 (NT3) (100 ng/ml; Peprotech). Medium was replaced every 2-3 days. These cells have been characterized in detail by Hick et al (25). Differentiated neurons were collected after 2, 5 or 7 weeks differentiation.

Cell treatment and apoptosis assays.

INS-1E cells were exposed to 0.5 mM oleate in RPMI 1640 medium containing 1% fetal bovine serum (FBS) and 0.75% FFA-free bovine serum albumin (BSA) **(**10). Primary β-cells and dispersed rat and human islet cells were exposed to 0.5 mM oleate in Ham's F-10 medium without serum and 1% charcoal-absorbed BSA (10, 61). The oleate stock solution (50 mM) was prepared by dissolving oleate (sodium salt, Sigma) in 90% ethanol (10, 62, 63). The chemical ER stressor brefeldin-A (an inhibitor of ER-to-Golgi vesicle transport) was used at a concentration of 0.1 μg/ml (10). The cell-permeable superoxide dismutase (SOD)/catalase mimetic (31-33) manganese (III) tetrakis(1-methyl-4-pyridyl) porphyrin pentachloride (MnTMPyP, Alexis Biochemicals) was used at a concentration of 25 μM, 4,5-dihydroxybenzene-1,3-disulfonate (Tiron, Sigma-Aldrich) at a concentration of 12.5 μM, the adenylyl cyclase stimulator forskolin at a concentration of 20 μM,, the GLP-1 analog exendin-4 and the GIP mimetic [D-Ala^2]-GIP at concentrations of 50 nM and 100 nM, respectively (10). In all treatments the control condition contained a similar concentration of the vehicle (ethanol, DMSO or PBS).

Apoptosis was determined by fluorescence microscopy after Hoechst 33342 (5 μg/ml; Sigma-Aldrich) and propidium iodide (5 μg/ml) staining (10), Western blotting for

cleaved caspase-3 (10, 61), and apoTox-Glo Triplex Assay (Promega) according to the manufacturer's instructions.

Analysis of H_2O_2 levels using HyPer vectors.

The pHyPerMito and pHyPerCyto eukaryotic expression vectors (Evrogen, Moscow, Russia) were used for mitochondrial and cytoplasmic expression of the fluorescent H_2O_2 sensor protein HyPer, as previously described (64). Stable clones of INS-1E cells expressing these vectors (INS-1E-HyPerMito and INS-1E-HyPerCyto), verified by fluorescence measurements, were transfected with a siRNA targeting rat frataxin (siFx). 48h after transfection the cells were treated or not for 24h with oleate or brefeldin. Mitochondrial or cytosolic H_2O_2 production was detected as HyPer oxidation, measured by fluorescence (475/427 nm excitation and 520 nm emission) in a Victor^2 1420 Multilabel Counter fluorescence reader (Perkin Elmer). The data were expressed as mean values of the F475/F427 ratio.

Estimation of hydroxyl radical formation.

Hydroxyl radical formation was estimated using the fluorescent dye 3'-(p-hydroxyphenyl) fluorescein (HPF) (Life Technologies) according to the manufacturer's instructions.

Mitochondrial glutathione redox state measurement.

The mitochondrial glutathione redox state was analyzed using the redox-sensitive fluorescent probe roGFP1 targeted to the mitochondria (mt-roGFP1). INS-1E cells were plated in glass coverslips and transfected with control or frataxin siRNA. 16h after transfection the cells were treated or not for 24h with 20 μM forskolin, and then

they were infected with an adenovirus encoding mt-roGFP1 under the control of the cytomegalovirus promoter (multiplicity of infection 25–50). After infection the cells were further cultured for 48h in the presence or absence of 20 μM forskolin. After culture, the coverslips were mounted at the bottom of a 37°C temperature-controlled chamber placed on the stage of an inverted microscope equipped with a 40x objective. Cells were perifused with bicarbonate-buffered Krebs solution containing 10 mM glucose at a flow rate of 1 ml/min. Cell fluorescence ratio ($\lambda_{exitation}$400/480 nm / $\lambda_{emission}$535 nm) was measured every 30s. After 20 min of perifusion, the cells were perifused with 10 µM dithiothreitol (DTT) to maximally reduce roGFP1 (set to 0%), followed by 100 µM aldrithiol to maximally oxidize it (set to 100%). The fluorescence ratio was expressed in percentage of the maximally reduced and the maximally oxidized forms of roGFP1 (normalized fluorescence ratio).

Catalase activity measurement.

Frataxin was knocked down by siRNA (see below) in control INS-1E cells or INS-1E cells stably overexpressing catalase inside the mitochondria. Catalase enzyme activity was measured by ultraviolet spectroscopy in control and catalase overexpressing cell lysates. The decomposition of H_2O_2 was monitored at 240 nm as previously described (65). One unit of catalase activity was defined as 1 μM of H_2O_2 per minute at 25°C.

RNA interference.

INS-1E cells, FACS-purified primary rat β-cells, and dispersed rat and human islet cells were transfected overnight with 30 nM control siRNA (Qiagen) or siRNAs targeting rat or human frataxin, rat DP5, Bim, Puma or Bad (all from Invitrogen), using Lipofectamine RNAiMAX (Invitrogen). The siRNAs targeting frataxin (10),

DP5 (66), Puma (67), Bim (68) and Bad (69) have been previously validated in β-cells. siRNA-lipid complexes were formed in Opti-MEM (Invitrogen) for 20 min as previously described (10). siRNA sequences and Lipofectamine concentrations are described in Supplementary Material, Tables S1 and S2.

Immunofluorescence.

Cytochrome c release was examined by immunofluorescence (66, 67). INS-1E cells plated on poly-lysine coated coverslips were transfected with control or frataxin siRNA. 16h after transfection cells were cultured for 48h in the presence of 25 μM MnTMPyP and then treated for 24h with oleate alone or combined with MnTMPyP. The cells were fixed with 4% formaldehyde (70), permeabilized with 0.1% Triton X-100, blocked with 3% FBS and incubated overnight at 4°C with mouse anti-cytochrome c (1:500, BD Biosciences). Alexa Fluor 488 goat anti-mouse IgG (H+L) (1:500, Molecular Probes, Invitrogen) was used as secondary antibody. Nuclei were stained with Hoechst 33342 and the slides analyzed by inverted fluorescence microscopy (Zeiss Axiovert 200, Oberkochen, Germany).

mRNA extraction and real-time PCR.

mRNA was isolated from INS-1E cells, primary rat β-cells and dispersed rat islet cells using the Dynabeads mRNA DIRECT kit (Invitrogen) and reverse transcribed as previously described (63, 71). Real-time PCR was performed using Rotor-Gene SyBR Green on a Rotor-Gene Q cycler (Qiagen) (72), or using Q SYBR Green Supermix (BIO-RAD) on a MyiQ2 instrument Single Color (BIO-RAD) (59, 63). Gene expression was calculated as copies/ml using the standard curve approach (73). Standards were prepared in conventional PCR. Expression values were corrected for

the expression of the reference gene GAPDH that was not modified by the experimental conditions. The primer sequences are provided in Supplementary Material, Tables S3 and S4.

Western blotting.

INS-1E cells, dispersed rat islet cells or iPSC-derived neurons were lysed in Laemmli buffer. Total extracts were resolved in 10-15% SDS-Page and transferred to nitrocellulose membrane. Immunoblotting was performed using antibodies against frataxin (Santa Cruz), cleaved caspase-3 (Cell Signaling), cleaved caspase-9 (Cell Signaling), α -tubulin (Sigma-Aldrich), total Bim (Cell Signaling), human P-Bad (Ser112, Cell Signaling), total Bad (Cell Signaling), Bcl-X_L (Cell Signaling), and Bcl-2 (Cell Signaling). Protein detection was done using horseradish peroxidase-conjugated secondary antibodies and SuperSignal West Femto chemiluminescence revealing reagent (Thermo Scientific). Immunoreactive bands were detected with a ChemiDoc XRS+ system and Image Lab software (BIO-RAD) (10). Protein levels were corrected for levels of α-tubulin.

Statistical analysis.

Data are shown as means ± SE. Non-normally distributed variables were log-transformed before statistical testing. Comparisons between groups were made by ANOVA followed by two-sided Student's paired t test with Bonferroni correction for multiple comparisons. Comparisons between iPSC-derived neurons from control and FRDA patients were made by unpaired t test. A p value <0.05 was considered statistically significant.

Acknowledgments

We thank Isabelle Millard, Michael Pangerl, Nathalie Pachera, Stephanie Mertens and Anyishai Musuaya from the ULB Center for Diabetes Research for excellent technical support, and the Flow Cytometry Facility of the Erasmus campus of the ULB and Christine Dubois for β-cell sorting.

This work was supported by the Fonds Erasme Olivia De Clercq, Belgium; the Phillip Bennett and Kyle Bryant Translational Research Award of the Friedreich Ataxia Research Alliance, USA; the European Union (projects BetaBat and EFACTS in the Framework Programme 7 of the European Community); Actions de Recherche Concertée de la Communauté Française (ARC) and Fonds National de la Recherche Scientifique (FNRS), Belgium. BA is fellow of the FRIA-FNRS and JCJ is Research Director of the FNRS.

Conflict of interest

The authors declare no conflict of interest.

References

1. Pandolfo, M. (2002) The molecular basis of Friedreich ataxia. *Adv. Exp. Med. Biol.,* **516,** 99-118.

2. Campuzano, V., Montermini, L., Molto, M.D., Pianese, L., Cossee, M., Cavalcanti, F., Monros, E., Rodius, F., Duclos, F., Monticelli, A. *et al.* (1996) Friedreich's ataxia: autosomal recessive disease caused by an intronic GAA triplet repeat expansion. *Science,* **271,** 1423-1427.

3. Koeppen, A.H. (2011) Friedreich's ataxia: pathology, pathogenesis, and molecular genetics. *J. Neurol. Sci.,* **303,** 1-12.

4. Pandolfo, M. (2009) Friedreich ataxia: the clinical picture. *J. Neurol.,* **256 Suppl 1,** 3-8.

5. Durr, A., Cossee, M., Agid, Y., Campuzano, V., Mignard, C., Penet, C., Mandel, J.L., Brice, A. and Koenig, M. (1996) Clinical and genetic abnormalities in patients with Friedreich's ataxia. *N. Engl. J. Med.,* **335,** 1169-1175.

6. Filla, A., DeMichele, G., Caruso, G., Marconi, R. and Campanella, G. (1990) Genetic data and natural history of Friedreich's disease: a study of 80 Italian patients. *J. Neurol.,* **237,** 345-351.

7. Finocchiaro, G., Baio, G., Micossi, P., Pozza, G. and di Donato, S. (1988) Glucose metabolism alterations in Friedreich's ataxia. *Neurology,* **38,** 1292-1296.

8. Akhlaghi, H., Corben, L., Georgiou-Karistianis, N., Bradshaw, J., Storey, E., Delatycki, M.B. and Egan, G.F. (2011) Superior cerebellar peduncle atrophy in Friedreich's ataxia correlates with disease symptoms. *Cerebellum,* **10,** 81-87.

9. Koeppen, A.H. and Mazurkiewicz, J.E. (2013) Friedreich ataxia: neuropathology revised. *J. Neuropathol. Exp. Neurol.,* **72,** 78-90.

10. Cnop, M., Igoillo-Esteve, M., Rai, M., Begu, A., Serroukh, Y., Depondt, C., Musuaya, A.E., Marhfour, I., Ladrière, L., Moles Lopez, X. *et al.* (2012) Central role and mechanisms of β-cell dysfunction and death in Friedreich ataxia–associated diabetes. *Ann. Neurol.,* **72,** 971-982.

11. Cnop, M., Mulder, H. and Igoillo-Esteve, M. (2013) Diabetes in Friedreich Ataxia. *J. Neurochem.,* **126** 94-102.

12. Schulz, J.B., Dehmer, T., Schols, L., Mende, H., Hardt, C., Vorgerd, M., Burk, K., Matson, W., Dichgans, J., Beal, M.F. *et al.* (2000) Oxidative stress in patients with Friedreich ataxia. *Neurology,* **55,** 1719-1721.

13. Chantrel-Groussard, K., Geromel, V., Puccio, H., Koenig, M., Munnich, A., Rotig, A. and Rustin, P. (2001) Disabled early recruitment of antioxidant defenses in Friedreich's ataxia. *Hum. Mol. Genet.,* **10,** 2061-2067.

14. Rotig, A., de Lonlay, P., Chretien, D., Foury, F., Koenig, M., Sidi, D., Munnich, A. and Rustin, P. (1997) Aconitase and mitochondrial iron-sulphur protein deficiency in Friedreich ataxia. *Nat. Genet.,* **17,** 215-217.

15. Bulteau, A.L., O'Neill, H.A., Kennedy, M.C., Ikeda-Saito, M., Isaya, G. and Szweda, L.I. (2004) Frataxin acts as an iron chaperone protein to modulate mitochondrial aconitase activity. *Science,* **305,** 242-245.

16. Armstrong, J.S., Khdour, O. and Hecht, S.M. (2010) Does oxidative stress contribute to the pathology of Friedreich's ataxia? A radical question. *Faseb J.,* **24,** 2152-2163.

17. Palomo, G.M., Cerrato, T., Gargini, R. and Diaz-Nido, J. (2011) Silencing of frataxin gene expression triggers p53-dependent apoptosis in human neuron-like cells. *Hum. Mol. Genet.,* **20,** 2807-2822.

18. Hotchkiss, R.S., Strasser, A., McDunn, J.E. and Swanson, P.E. (2009) Cell death. *N. Engl. J. Med.,* **361,** 1570-1583.

19. Gurzov, E.N. and Eizirik, D.L. (2011) Bcl-2 proteins in diabetes: mitochondrial pathways of beta-cell death and dysfunction. *Trends Cell Biol.,* **21,** 424-431.

20. Kim, H., Rafiuddin-Shah, M., Tu, H.C., Jeffers, J.R., Zambetti, G.P., Hsieh, J.J. and Cheng, E.H. (2006) Hierarchical regulation of mitochondrion-dependent apoptosis by BCL-2 subfamilies. *Nat. Cell Biol.,* **8,** 1348-1358.

21. Brunelle, J.K. and Letai, A. (2009) Control of mitochondrial apoptosis by the Bcl-2 family. *J. Cell Sci.,* **122,** 437-441.

22. Ku, S., Soragni, E., Campau, E., Thomas, E.A., Altun, G., Laurent, L.C., Loring, J.F., Napierala, M. and Gottesfeld, J.M. (2010) Friedreich's ataxia induced pluripotent stem cells model intergenerational GAATTC triplet repeat instability. *Cell Stem Cell,* **7,** 631-637.

23. Liu, J., Verma, P.J., Evans-Galea, M.V., Delatycki, M.B., Michalska, A., Leung, J., Crombie, D., Sarsero, J.P., Williamson, R., Dottori, M. *et al.* (2011) Generation of induced pluripotent stem cell lines from Friedreich ataxia patients. *Stem Cell Rev,* **7,** 703-713.

24. Du, J., Campau, E., Soragni, E., Ku, S., Puckett, J.W., Dervan, P.B. and Gottesfeld, J.M. (2012) Role of mismatch repair enzymes in GAA.TTC triplet-repeat expansion in Friedreich ataxia induced pluripotent stem cells. *J. Biol. Chem.,* **287,** 29861-29872.

25. Hick, A., Wattenhofer-Donze, M., Chintawar, S., Tropel, P., Simard, J.P., Vaucamps, N., Gall, D., Lambot, L., Andre, C., Reutenauer, L. *et al.* (2013) Neurons and cardiomyocytes derived from induced pluripotent stem cells as a

model for mitochondrial defects in Friedreich's ataxia. *Dis. Model. Mech.,* **6,** 608-621.

26. Wong, A., Yang, J., Cavadini, P., Gellera, C., Lonnerdal, B., Taroni, F. and Cortopassi, G. (1999) The Friedreich's ataxia mutation confers cellular sensitivity to oxidant stress which is rescued by chelators of iron and calcium and inhibitors of apoptosis. *Hum. Mol. Genet.,* **8,** 425-430.

27. Anderson, P.R., Kirby, K., Orr, W.C., Hilliker, A.J. and Phillips, J.P. (2008) Hydrogen peroxide scavenging rescues frataxin deficiency in a Drosophila model of Friedreich's ataxia. *Proc. Natl. Acad. Sci. U. S. A.,* **105,** 611-616.

28. Pandolfo, M. (2008) Drug Insight: antioxidant therapy in inherited ataxias. *Nat. Clin. Pract. Neurol.,* **4,** 86-96.

29. Roma, L.P., Duprez, J., Takahashi, H.K., Gilon, P., Wiederkehr, A. and Jonas, J.C. (2012) Dynamic measurements of mitochondrial hydrogen peroxide concentration and glutathione redox state in rat pancreatic beta-cells using ratiometric fluorescent proteins: confounding effects of pH with HyPer but not roGFP1. *Biochem. J.,* **441,** 971-978.

30. Roma, L.P., Pascal, S.M., Duprez, J. and Jonas, J.C. (2012) Mitochondrial oxidative stress contributes differently to rat pancreatic islet cell apoptosis and insulin secretory defects after prolonged culture in a low non-stimulating glucose concentration. *Diabetologia,* **55,** 2226-2237.

31. Gardner, P.R., Nguyen, D.D. and White, C.W. (1996) Superoxide scavenging by Mn(II/III) tetrakis (1-methyl-4-pyridyl) porphyrin in mammalian cells. *Arch. Biochem. Biophys.,* **325,** 20-28.

32. Mortensen, J., Shames, B., Johnson, C.P. and Nilakantan, V. (2011) MnTMPyP, a superoxide dismutase/catalase mimetic, decreases inflammatory indices in ischemic acute kidney injury. *Inflamm. Res.,* **60,** 299-307.

33. Liang, H.L., Hilton, G., Mortensen, J., Regner, K., Johnson, C.P. and Nilakantan, V. (2009) MnTMPyP, a cell-permeant SOD mimetic, reduces oxidative stress and apoptosis following renal ischemia-reperfusion. *Am. J. Physiol. Renal. Physiol.,* **296,** F266-276.

34. Han, Y.H. and Park, W.H. (2009) Tiron, a ROS scavenger, protects human lung cancer Calu-6 cells against antimycin A-induced cell death. *Oncol. Rep.,* **21,** 253-261.

35. Kim, H., Tu, H.C., Ren, D., Takeuchi, O., Jeffers, J.R., Zambetti, G.P., Hsieh, J.J. and Cheng, E.H. (2009) Stepwise activation of BAX and BAK by tBID, BIM, and PUMA initiates mitochondrial apoptosis. *Mol. Cell,* **36,** 487-499.

36. Youle, R.J. and Strasser, A. (2008) The BCL-2 protein family: opposing activities that mediate cell death. *Nat. Rev. Mol. Cell. Biol.,* **9,** 47-59.

37. Weber, A., Paschen, S.A., Heger, K., Wilfling, F., Frankenberg, T., Bauerschmitt, H., Seiffert, B.M., Kirschnek, S., Wagner, H. and Hacker, G.

(2007) BimS-induced apoptosis requires mitochondrial localization but not interaction with anti-apoptotic Bcl-2 proteins. *J. Cell Biol.,* **177,** 625-636.

38. Al-Mahdawi, S., Pinto, R.M., Ismail, O., Varshney, D., Lymperi, S., Sandi, C., Trabzuni, D. and Pook, M. (2008) The Friedreich ataxia GAA repeat expansion mutation induces comparable epigenetic changes in human and transgenic mouse brain and heart tissues. *Hum. Mol. Genet.,* **17,** 735-746.

39. Jiralerspong, S., Ge, B., Hudson, T.J. and Pandolfo, M. (2001) Manganese superoxide dismutase induction by iron is impaired in Friedreich ataxia cells. *FEBS Lett.,* **509,** 101-105.

40. Ristow, M., Mulder, H., Pomplun, D., Schulz, T.J., Muller-Schmehl, K., Krause, A., Fex, M., Puccio, H., Muller, J., Isken, F. *et al.* (2003) Frataxin deficiency in pancreatic islets causes diabetes due to loss of ◘ cell mass. *J. Clin. Invest.,* **112,** 527-534.

41. Pandolfo, M. (2012) Friedreich ataxia: new pathways. *J. Child Neurol.,* **27,** 1204-1211.

42. Hua, H., Shang, L., Martinez, H., Freeby, M., Gallagher, M.P., Ludwig, T., Deng, L., Greenberg, E., Leduc, C., Chung, W.K. *et al.* (2013) iPSC-derived beta cells model diabetes due to glucokinase deficiency. *J. Clin. Invest.,* **123,** 3146-3153.

43. Kearney, M., Orrell, R.W., Fahey, M. and Pandolfo, M. (2012) Antioxidants and other pharmacological treatments for Friedreich ataxia. *Cochrane Database Syst. Rev.,* **4,** CD007791.

44. Kamat, C.D., Gadal, S., Mhatre, M., Williamson, K.S., Pye, Q.N. and Hensley, K. (2008) Antioxidants in central nervous system diseases: preclinical promise and translational challenges. *J. Alzheimers Dis.,* **15,** 473-493.

45. Brewer, G.J. (2010) Why vitamin E therapy fails for treatment of Alzheimer's disease. *J. Alzheimers Dis.,* **19,** 27-30.

46. Li, N., Li, B., Brun, T., Deffert-Delbouille, C., Mahiout, Z., Daali, Y., Ma, X.J., Krause, K.H. and Maechler, P. (2012) NADPH oxidase NOX2 defines a new antagonistic role for reactive oxygen species and cAMP/PKA in the regulation of insulin secretion. *Diabetes,* **61,** 2842-2850.

47. Holst, J.J., Burcelin, R. and Nathanson, E. (2011) Neuroprotective properties of GLP-1: theoretical and practical applications. *Curr. Med. Res. Opin.,* **27,** 547-558.

48. Li, Y., Chigurupati, S., Holloway, H.W., Mughal, M., Tweedie, D., Bruestle, D.A., Mattson, M.P., Wang, Y., Harvey, B.K., Ray, B. *et al.* (2012) Exendin-4 ameliorates motor neuron degeneration in cellular and animal models of amyotrophic lateral sclerosis. *PLoS One,* **7,** e32008.

49. McClean, P.L., Parthsarathy, V., Faivre, E. and Holscher, C. (2011) The diabetes drug liraglutide prevents degenerative processes in a mouse model of Alzheimer's disease. *J. Neurosci.,* **31,** 6587-6594.

50. Li, Y., Perry, T., Kindy, M.S., Harvey, B.K., Tweedie, D., Holloway, H.W., Powers, K., Shen, H., Egan, J.M., Sambamurti, K. *et al.* (2009) GLP-1 receptor stimulation preserves primary cortical and dopaminergic neurons in cellular and rodent models of stroke and Parkinsonism. *Proc. Natl. Acad. Sci. U. S. A.,* **106,** 1285-1290.

51. Martin, B., Golden, E., Carlson, O.D., Pistell, P., Zhou, J., Kim, W., Frank, B.P., Thomas, S., Chadwick, W.A., Greig, N.H. *et al.* (2009) Exendin-4 improves glycemic control, ameliorates brain and pancreatic pathologies, and extends survival in a mouse model of Huntington's disease. *Diabetes,* **58,** 318-328.

52. Briyal, S., Gulati, K. and Gulati, A. (2012) Repeated administration of exendin-4 reduces focal cerebral ischemia-induced infarction in rats. *Brain Res.,* **1427,** 23-34.

53. Darsalia, V., Mansouri, S., Ortsater, H., Olverling, A., Nozadze, N., Kappe, C., Iverfeldt, K., Tracy, L.M., Grankvist, N., Sjoholm, A. *et al.* (2012) Glucagon-like peptide-1 receptor activation reduces ischaemic brain damage following stroke in Type 2 diabetic rats. *Clin. Sci. (Lond.),* **122,** 473-483.

54. Asfari, M., Janjic, D., Meda, P., Li, G., Halban, P.A. and Wollheim, C.B. (1992) Establishment of 2-mercaptoethanol-dependent differentiated insulin-secreting cell lines. *Endocrinology,* **130,** 167-178.

55. Ortis, F., Cardozo, A.K., Crispim, D., Storling, J., Mandrup-Poulsen, T. and Eizirik, D.L. (2006) Cytokine-induced proapoptotic gene expression in insulin-producing cells is related to rapid, sustained, and nonoscillatory nuclear factor-| B activation. *Mol. Endocrinol.,* **20,** 1867-1879.

56. Ling, Z., Hannaert, J.C. and Pipeleers, D. (1994) Effect of nutrients, hormones and serum on survival of rat islet β-cells in culture. *Diabetologia,* **37,** 15-21.

57. Lupi, R., Dotta, F., Marselli, L., Del Guerra, S., Masini, M., Santangelo, C., Patane, G., Boggi, U., Piro, S., Anello, M. *et al.* (2002) Prolonged exposure to free fatty acids has cytostatic and pro-apoptotic effects on human pancreatic islets: evidence that beta-cell death is caspase mediated, partially dependent on ceramide pathway, and Bcl-2 regulated. *Diabetes,* **51,** 1437-1442.

58. Moore, F., Colli, M.L., Cnop, M., Esteve, M.I., Cardozo, A.K., Cunha, D.A., Bugliani, M., Marchetti, P. and Eizirik, D.L. (2009) PTPN2, a candidate gene for type 1 diabetes, modulates interferon-γ-induced pancreatic β-cell apoptosis. *Diabetes,* **58,** 1283-1291.

59. Igoillo-Esteve, M., Marselli, L., Cunha, D.A., Ladriere, L., Ortis, F., Grieco, F.A., Dotta, F., Weir, G.C., Marchetti, P., Eizirik, D.L. *et al.* (2010) Palmitate induces a pro-inflammatory response in human pancreatic islets that mimics

CCL2 expression by beta cells in type 2 diabetes. *Diabetologia,* **53,** 1395-1405.

60. Dottori, M. and Pera, M.F. (2008) Neural differentiation of human embryonic stem cells. *Methods Mol. Biol.,* **438,** 19-30.

61. Cunha, D.A., Ladriere, L., Ortis, F., Igoillo-Esteve, M., Gurzov, E.N., Lupi, R., Marchetti, P., Eizirik, D.L. and Cnop, M. (2009) Glucagon-like peptide-1 agonists protect pancreatic β-cells from lipotoxic endoplasmic reticulum stress through upregulation of BiP and JunB. *Diabetes,* **58,** 2851-2862.

62. Cnop, M., Hannaert, J.C., Hoorens, A., Eizirik, D.L. and Pipeleers, D.G. (2001) Inverse relationship between cytotoxicity of free fatty acids in pancreatic islet cells and cellular triglyceride accumulation. *Diabetes,* **50,** 1771-1777.

63. Cunha, D.A., Hekerman, P., Ladriere, L., Bazarra-Castro, A., Ortis, F., Wakeham, M.C., Moore, F., Rasschaert, J., Cardozo, A.K., Bellomo, E. *et al.* (2008) Initiation and execution of lipotoxic ER stress in pancreatic β-cells. *J. Cell Sci.,* **121,** 2308-2318.

64. Gurgul-Convey, E., Mehmeti, I., Lortz, S. and Lenzen, S. (2011) Cytokine toxicity in insulin-producing cells is mediated by nitro-oxidative stress-induced hydroxyl radical formation in mitochondria. *J. Mol. Med. (Berl.),* **89,** 785-798.

65. Gurgul, E., Lortz, S., Tiedge, M., Jorns, A. and Lenzen, S. (2004) Mitochondrial catalase overexpression protects insulin-producing cells against toxicity of reactive oxygen species and proinflammatory cytokines. *Diabetes,* **53,** 2271-2280.

66. Gurzov, E.N., Ortis, F., Cunha, D.A., Gosset, G., Li, M., Cardozo, A.K. and Eizirik, D.L. (2009) Signaling by IL-1β+IFN-γ and ER stress converge on DP5/Hrk activation: a novel mechanism for pancreatic β-cell apoptosis. *Cell Death Differ.,* **16,** 1539-1550.

67. Gurzov, E.N., Germano, C.M., Cunha, D.A., Ortis, F., Vanderwinden, J.M., Marchetti, P., Zhang, L. and Eizirik, D.L. (2010) p53 up-regulated modulator of apoptosis (PUMA) activation contributes to pancreatic beta-cell apoptosis induced by proinflammatory cytokines and endoplasmic reticulum stress. *J. Biol. Chem.,* **285,** 19910-19920.

68. Barthson, J., Germano, C.M., Moore, F., Maida, A., Drucker, D.J., Marchetti, P., Gysemans, C., Mathieu, C., Nunez, G., Jurisicova, A. *et al.* (2011) Cytokines tumor necrosis factor-alpha and interferon-gamma induce pancreatic beta-cell apoptosis through STAT1-mediated Bim protein activation. *J. Biol. Chem.,* **286,** 39632-39643.

69. Cunha, D.A., Gurzov, E.N., Naamane, N., Ortis, F., Cardozo, A.K., Bugliani, M., Marchetti, P., Eizirik, D.L. and Cnop, M. (2014) JunB protects beta-cells

from lipotoxicity via the XBP1-AKT pathway. *Cell Death Differ.,* **21,** 1313-1324.

70. Ladriere, L., Igoillo-Esteve, M., Cunha, D.A., Brion, J.P., Bugliani, M., Marchetti, P., Eizirik, D.L. and Cnop, M. (2010) Enhanced signaling downstream of ribonucleic acid-activated protein kinase-like endoplasmic reticulum kinase potentiates lipotoxic endoplasmic reticulum stress in human islets. *J. Clin. Endocrinol. Metab.,* **95,** 1442-1449.

71. Rasschaert, J., Ladriere, L., Urbain, M., Dogusan, Z., Katabua, B., Sato, S., Akira, S., Gysemans, C., Mathieu, C. and Eizirik, D.L. (2005) Toll-like receptor 3 and STAT-1 contribute to double-stranded RNA+ interferon-γ-induced apoptosis in primary pancreatic β-cells. *J. Biol. Chem.,* **280,** 33984-33991.

72. Igoillo-Esteve, M., Genin, A., Lambert, N., Désir, J., Pirson, I., Abdulkarim, B., Simonis, N., Drielsma, A., Marselli, L., Marchetti, P. *et al.* (2013) tRNA methyltransferase homolog gene TRMT10A mutation in young onset diabetes and primary microcephaly in humans. *PLoS Genet*. DOI: 10.1371/journal.pgen.1003888

73. Overbergh, L., Valckx, D., Waer, M. and Mathieu, C. (1999) Quantification of murine cytokine mRNAs using real time quantitative reverse transcriptase PCR. *Cytokine,* **11,** 305-312.

Legends to Figures

Figure 1. Frataxin deficiency induces mitochondrial oxidative stress in β-cells.

INS-1E cells were transfected with control siRNA (siCT) or siRNA targeting rat frataxin (siFx). Frataxin and SOD2 mRNA expression was measured by real-time PCR and expressed as fold of siCT (A and D). Frataxin protein expression was examined by Western blot and normalized to the expression of α-tubulin (B). Apoptosis was evaluated by Hoechst 33342/propidium iodide staining (C). (E and F) INS-1E cells were transfected with siCT or siFx together with the expression vector HyPerMito or HyPerCyto, coding for the fluorescent H_2O_2 sensor protein HyPer targeted to the mitochondria or the cytosol, respectively. 48h after transfection the cells were treated or not (CT) for 24h with oleate (OL, 0.5 mM) or brefeldin (BR, 0.1 μg/ml). HyPer oxidation, measured by fluorescence count reader (F475/F427), was used as indicative of mitochondrial or cytosolic H_2O_2 production. Hydroxyl radical formation, estimated by fluorescent HPF, was examined in frataxin expressing (siCT) of frataxin deficient (siFx) INS-1E cells treated or not with OL or BR for 24h (G). Mitochondrial glutathione redox state was analyzed using the redox-sensitive fluorescent probe roGFP1 targeted to the mitochondria (mt-roGFP1). Frataxin deficient (siFx) or frataxin competent (siCT) in INS-1E cells were infected with an adenovirus encoding mt-roGFP1. 48h after infection the cells were perifused with buffered Krebs solution containing 10 mM glucose and mitochondrial glutathione redox state was assessed by measuring the mt-roGFP1 fluorescence ratio (λ_{ex}400/480 nm/λ_{em}535 nm). The results were normalized to the maximally reduced and maximally oxidized mt-roGFP1 fluorescence ratio following cell perifusion with DTT and aldrithiol, respectively (H). Results are means ± SE of 3-8 independent

experiments. * Treated vs CT, *p<0.05, ** p<0.01, *** p<0.001; § siFx vs siCT, § p<0.05, §§ p<0.01, by paired t test.

Figure 2. ROS scavenging partially prevents apoptosis in frataxin-deficient β-cells. INS-1E cells or dispersed rat islet cells were transfected with control siRNA (siCT) or siRNA targeting frataxin (siFx). 16h after transfection the cells were exposed or not for 48h to the ROS scavengers MnTMPyP (25 μM), or 4,5-dihydroxybenzene-1,3-disulfonate (Tiron, 12.5 μM) and then treated or not (CT) for 24h with oleate (OL, 0.5 mM), or brefeldin (BR, 0.1 μg/ml), alone or combined with MnTMPyP or Tiron. Apoptosis was examined by Hoechst 33342/propidium iodide staining (A, D, F, INS-1E cells; E, dispersed rat islet cells), or Western blots for cleaved caspase-3 (B), quantified by densitometry and normalized to α-tubulin (C). (G) Frataxin was silenced in wild type or mitochondrial catalase-overexpressing INS-1E cells (Mito Cat). Cells were then treated for 24h with brefeldin (BR). Caspase-3 activation was measured using the ApoTox kit. Results are means ± SE of 3-5 independent experiments. * Treated vs CT, *p<0.05, ** p<0.01, *** p<0.001; § siFx vs siCT, § p<0.05, §§ p<0.01, §§§ p<0.001; # presence vs absence of MnTMPyP or wild type vs Mito Cat INS-1E cells, # p<0.05, by paired ratio t test.

Figure 3. Frataxin deficiency activates the intrinsic pathway of apoptosis in β-cells. INS-1E cells were transfected with control siRNA (siCT) or siRNA targeting frataxin (siFx). 48h after transfection the cells were treated or not (CT) with oleate (OL, 0.5 mM) for 24h. Cytochrome c release was evaluated by immunofluorescence. Representative pictures are shown in (A). Arrows indicate cells with diffuse cytoplasmic staining for cytochrome c. (B) Quantification of A (n=4-5). More than

900 cells were counted in each experiment. (C-E) DP5, Bim and Puma expression, caspase-3 activation and BAD phosphorylation were examined 72h after frataxin knockdown. DP5, Puma and Bim mRNA expression was measured by real-time PCR and corrected for the reference gene GAPDH (C). Caspase-3 activation, Bim protein expression and BAD phosphorylation were examined by Western blot (D). (E) Densitometry of D. Results are means ± SE of 3-9 independent experiments. * Treated vs CT, * $p<0.05$, ** $p<0.01$; § siFx vs siCT, § $p<0.05$, §§ $p<0.01$, by paired t test.

Figure 4. Oxidative stress activates the intrinsic pathway of apoptosis in frataxin-deficient β-cells. Frataxin was silenced in INS-1E cells by siRNA (siFx). 16h after transfection the cells were cultured in the absence (CT) or presence of MnTMPyP (25 mM) for 48h. The cells were then treated or not (CT) with oleate (OL, 0.5 mM) alone or combined with MnTMPyP for 24h. Cytochrome c release was evaluated by immunofluorescence. (A) Representative pictures are shown. Arrows indicate cells with diffuse cytoplasmic cytochrome c staining. (B) Quantification of A. More than 900 cells were counted in each experiment. Results are means ± SE of 5 independent experiments. * Treated vs CT, $p<0.05$; # presence vs absence of MnTMPyP; # $p<0.05$, ### $p<0.001$, by paired t test.

Figure 5. BAD, DP5 and Bim but not Puma mediate apoptosis in frataxin-deficient β-cells. Frataxin was silenced (siFx) or not (siCT) in INS-1E cells (A, B, D, E, G, H, J, K) and primary rat β-cells (C, F, I) alone or combined with BAD (A-C), DP5 (D-F), Bim (G-I) or Puma siRNA (J-K). Cells were then treated or not (CT) for 24h with oleate (OL, 0.5 mM) or brefeldin (BR, 0.1 µl/ml). Apoptosis was evaluated

by Hoechst 33342/propidium iodide staining. Results are means ± SE of 3-4 independent experiments. * Treated vs CT, * $p<0.05$, ** $p<0.01$; § siFx vs siCT, §$p<0.05$, §§ $p<0.01$; # siFx vs double knockdown, # $p<0.05$, ## $p<0.01$, ### $p<0.001$, by paired t test or ANOVA followed by paired t test with Bonferroni correction for multiple comparisons.

Figure 6. The intrinsic pathway of apoptosis is activated in iPSC-derived neurons from FRDA patients. Caspase-3 and -9 activation, Bim and frataxin expression were examined by Western blot (A) in iPSC-derived neurons (2 and 5 weeks differentiation) from one healthy control (CT) and two FRDA patients (FA 1 and 2), two clones of each (indicated as A and B). (B-E) Densitometry of A. Symbols represent independent experiments. *FRDA vs CT, * $p<0.05$, ** $p<0.01$, *** $p<0.001$, by unpaired t test.

Figure 7. Forskolin reduces oxidative stress and prevents activation of the intrinsic pathway of apoptosis in frataxin-deficient β-cells and iPSC-derived neurons from FRDA patients. Mitochondrial H_2O_2 production was measured using the H_2O_2 fluorescent sensor HyPer targeted to the mitochondria (HyPerMito). Frataxin was silenced (siFx) or not (siCT) in INS-1E cells together with the expression vector HyPerMito, 48h after transfection the cells were treated or not (CT) for 24h with 20 μM forskolin (FK). HyPer oxidation, measured by fluorescence count reader (F475/F427), was used as indicative of mitochondrial H_2O_2 production. The results are means ± SE of 7 independent experiments (A). Mitochondrial glutathione redox state was analyzed using the redox-sensitive fluorescent probe roGFP1 targeted to the mitochondria (mt-roGFP1). Frataxin was silenced or not in INS-1E cells. 16h

after transfection the cells were treated or not (CT) for 24h with 20 μM forskolin (FK), and then infected with an adenovirus encoding mt-roGFP1. After infection, the cells were further treated or not with forskolin for 48h. The cells were then perifused with buffered Krebs solution containing 10 mM glucose and mitochondrial glutathione redox state was assessed by measuring the mt-roGFP1 fluorescence ratio (λ_{ex}400/480 nm/λ_{em}535 nm). The results (means ± SE of 3 independent experiments) were normalized to the maximally reduced and maximally oxidized mt-roGFP1 fluorescence ratio following cell perifusion with DTT and aldrithiol, respectively (B). INS-1E (C-F) and dispersed rat islet cells (G-H) were transfected with siCT or siFx and 48h later treated or not (CT) for 24h with brefeldin (BR, 0.1 μl/ml) alone or combined with forskolin (FK, 20 μM). Western blots for caspase-3 activation and Bad phosphorylation were used to assess apoptosis in INS-1E cells. (C) Representative blot and (D-E) densitometry of the Western blots (n=4 independent experiments). P-Bad was normalized to total Bad and cleaved caspase-3 to α-tubulin. In dispersed rat islet cells apoptosis was examined by Hoechst 33342/propidium iodide staining (G). Bim mRNA expression in INS-1E cells (F) and dispersed islets (H) was measured by real-time PCR and corrected for the reference gene GAPDH. Results are means ± SE of 3-4 independent experiments. iPSC-derived neurons from two FRDA patients (FA 1 and 2), two clones of each (indicated as A and B) (5 and 7 weeks differentiation), were cultured for 72h in the absence (CT) or presence of 20 μM forskolin (FK). Densitometry of the Western blots for caspase-3 cleavage (I-J) and Bim_L + Bim_S expression (K-L). Symbols represent independent experiments. All observations for the 4 clones were pooled in panels J and L. * Treated vs CT, * $p<0.05$, ** $p<0.01$; § siFx vs siCT, § $p<0.05$, §§§ $p<0.001$; # with FK vs without FK, # $p<0.05$, ## $p<0.01$, by ratio t test.

Abbreviations: DTT, dithiothreitol; ER, endoplasmic reticulum; FFA, free fatty acid; FRDA, Friedreich's ataxia; GIP, glucose-dependent inhibitory peptide; GLP-1, glucagon-like peptide-1; GSH, reduced glutathione; iPSC, induced pluripotent stem cell; ROS, reactive oxygen species; SOD, superoxide dismutase.

Figure 1

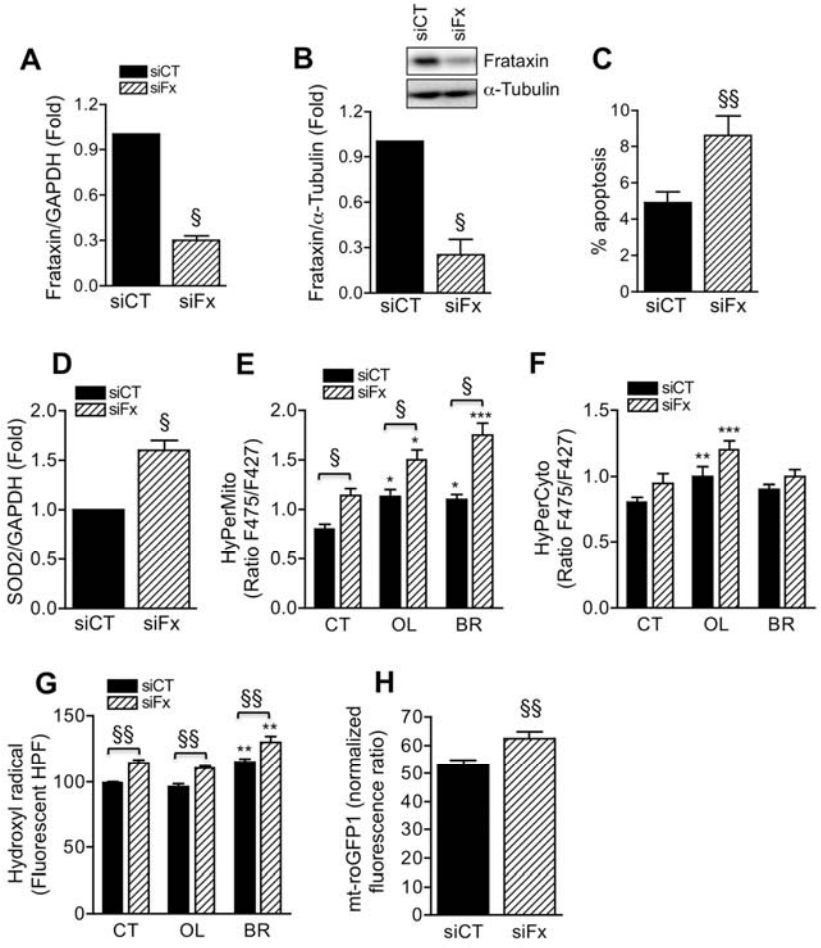

Figure 2

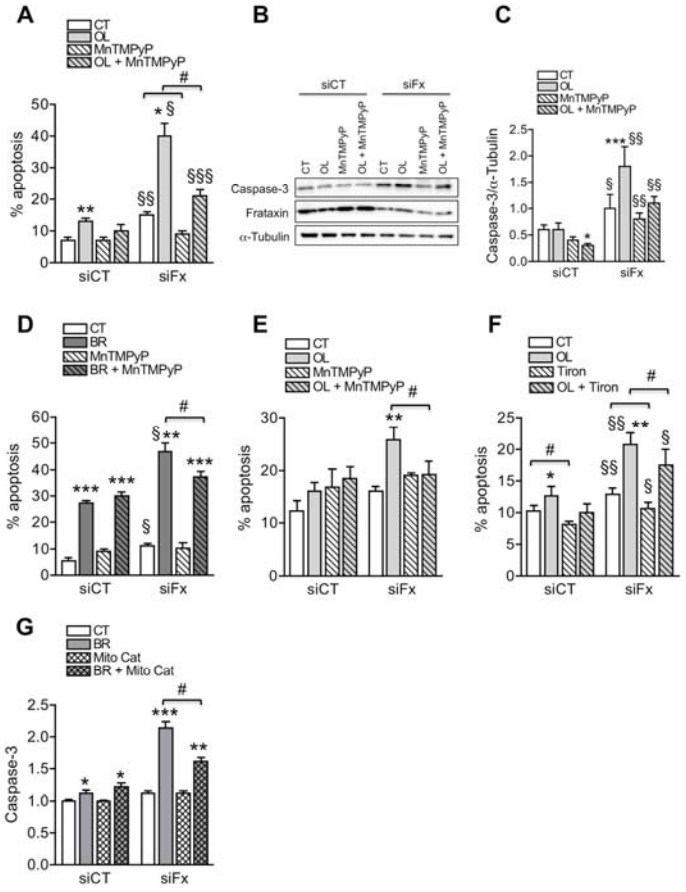

Figure 3

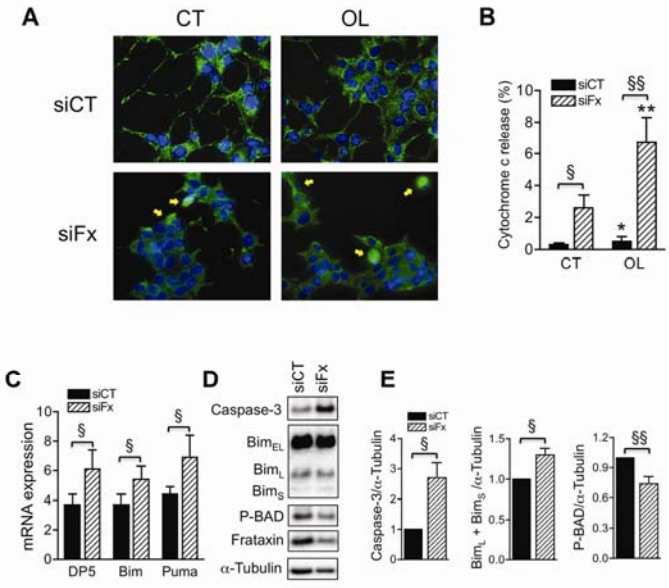

Figure 4

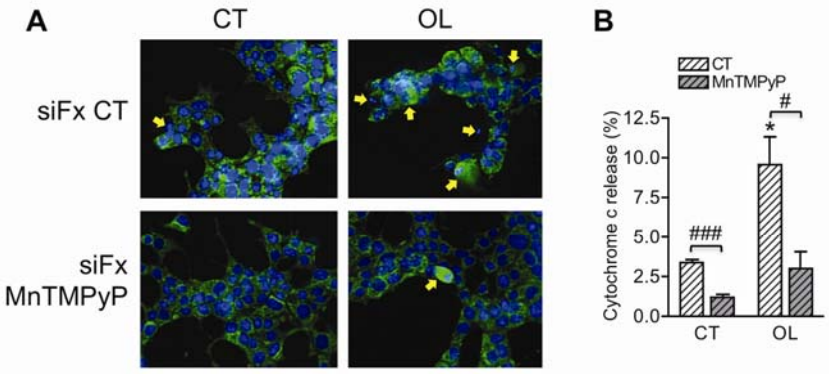

Figure 5

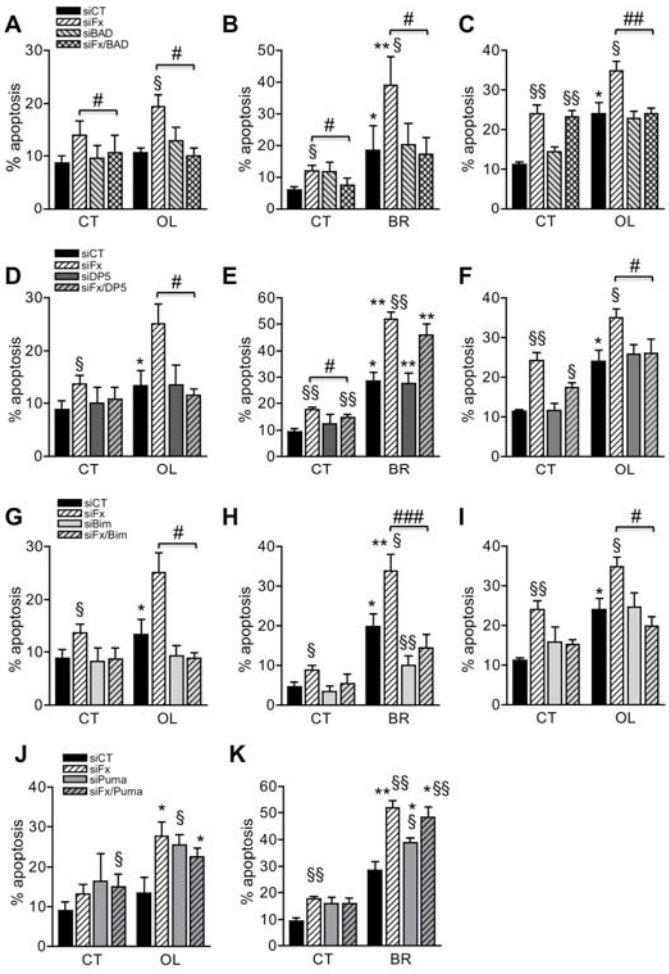

Figure 6

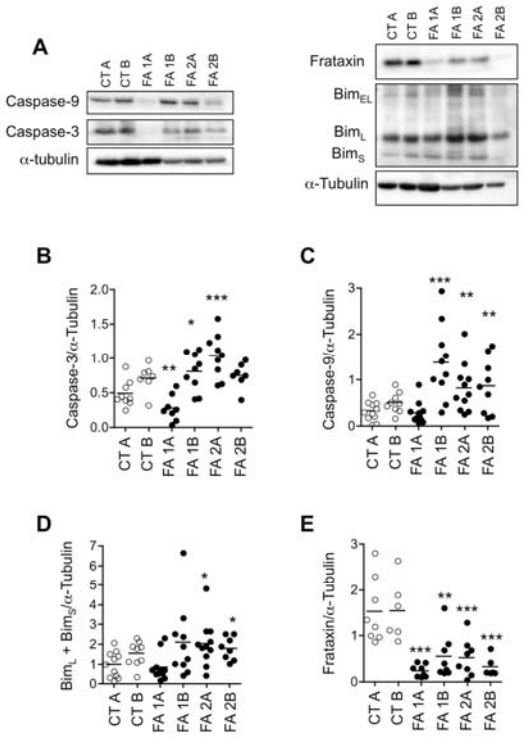

Figure 7